Research Square

Preprints are preliminary reports that have not undergone peer review.
They should not be considered conclusive, used to inform clinical practice,
or referenced by the media as validated information.

Chronic β-catenin O-GlcNAcylation is a driver of hypertrophy in diabetic cardiomyopathy

Simon Ducheix
Institut du Thorax
Natacha Fourny
UCLouvain
Michael Joubert
Université de Caen Normandie
David Montaigne
Institut Pasteur de Lille
Romain Capoulade
Institut du Thorax
Pascal Aumond
Institut du Thorax
Gilles Toumaniantz
Institut du Thorax
Laura Guilbert
UCLouvain
Rola Shaaban
Institut du Thorax
Abdelouhab Bouaboud
Institut Cochin
Virginie Salnot
Institut Cochin
Samuel Frey
Institut du Thorax
Thibaud Sotin
Institut du Thorax
Gilliane Chadeuf
Institut du Thorax
Bart Staels
Institut Pasteur de Lille
Cedric Le May
Institut du Thorax
Bertrand Cariou

Institut du Thorax

Mikael Croyal

Institut du Thorax

Samy Hadjadj

Institut du Thorax

Tarik Issad

Institut Cochin

Luc Bertrand

UCLouvain

Xavier Prieur

xavier.prieur@univ-nantes.fr

Institut du Thorax

Research Article

Keywords:

Posted Date: July 23rd, 2026

DOI: https://doi.org/10.21203/rs.3.rs-10392150/v1

License: This work is licensed under a Creative Commons Attribution 4.0 International License.
Read Full License

Additional Declarations: No competing interests reported.

Abstract

Background

The incidence of heart failure is approximately 2.5-fold higher in patients with type 2 diabetes than in non-diabetic individuals. Diabetic cardiomyopathy is characterized by diastolic dysfunction and left ventricular hypertrophy. The diabetic heart exhibits insulin resistance, leading to impaired glucose uptake and oxidation and, consequently, to intracellular glucose overload and glucotoxic stress. To further investigate the mechanisms underlying diabetic cardiomyopathy, we have previously examined the cardiac phenotype of lipodystrophic and severely insulin-resistant seipin knockout mice. These mice developed left ventricular hypertrophy associated with chronic activation of the hexosamine biosynthetic pathway, which promotes over-O-GlcNAcylation of cardiac proteins.

Methods

To assess the causal role of chronic activation of the hexosamine biosynthetic pathway in cardiac dysfunction in seipin knockout mice, we used adeno-associated virus-mediated cardiac overexpression of O-GlcNAcase, the enzyme responsible for removing O-GlcNAc moieties. Cardiac properties were evaluated by echocardiography. O-GlcNAcylated proteins were enriched using wheat germ agglutinin pull-down followed by proteomic analysis. Pharmacological inhibition and genetic modulation were used to investigate the role of β-catenin signalling.

Results

Cardiac overexpression of O-GlcNAcase corrected cardiac hypertrophy, as assessed by echocardiography, and improved insulin sensitivity in seipin knockout hearts. Proteomic analyses identified 28 proteins with increased O-linked N-acetylglucosamine modification in seipin knockout mice. Among these, β-catenin emerged as a candidate mediator, as expression of its target genes was increased in seipin knockout mice and normalized upon O-GlcNAcase overexpression. Increased β-catenin activity was associated with enhanced O-GlcNAcylation. Pharmacological inhibition of β-catenin using ICG-001 prevented cardiac hypertrophy in seipin knockout mice. Increased β-catenin O-GlcNAcylation and activity were also observed in two other murine models of diabetic cardiomyopathy. Selective enhancement of β-catenin O-GlcNAcylation was sufficient to induce hypertrophy in cultured cardiomyocytes.

Conclusion

These findings indicate that β-catenin O-GlcNAcylation contributes to cardiac remodelling in insulin-resistant states. This mechanism may extend beyond the seipin deficient specific model and could

represent a potential target for the treatment of cardiac hypertrophy associated with type 2 diabetes.

Research Insights

Question	Response
What is currently known about this topic?	Seipin-deficient mice develop cardiac hypertrophy and insulin resistance associated with increased O-GlcNAcylation levels.
What is the key research question?	Does chronic over-O-GlcNAcylation of cardiac protein drive cardiac dysfunction in this model?
What is new?	O-GlcNAcase overexpression reduces hypertrophy.
	β-catenin is hyper- O-GlcNAcylated and transcriptionally active.
	β-catenin inhibition prevents hypertrophy in vivo and β-catenin hyper-O-GlcNAcylation increases cardiomyocaytes size in vitro.
How might this study influence clinical practice?	Targeting β-catenin O-GlcNAcylation may limit cardiac hypertrophy in diabetes.

INTRODUCTION

The incidence of heart failure (HF) (1) is approximately 2.5-fold higher in patients with type 2 diabetes (T2D) than in non-diabetic individuals (2). Ischemic heart disease and hypertension are frequently associated with HF (3); nevertheless, a subset of diabetic patients develop HF in the absence of coronary artery or macrovascular disease, leading to the definition of diabetic cardiomyopathy (DCM) (4). DCM is characterized by diastolic dysfunction and left ventricular hypertrophy (LVH) (5, 6). In a large cohort, Iribarren and colleagues reported that each one-percentage-point increase in glycated hemoglobin (HbA1c) was associated with an independent 8% higher risk of HF-related death or hospitalization (7). Mechanistically, accumulating evidence indicates that alterations in cardiac substrate utilization and metabolic inflexibility are central features of DCM pathophysiology (5, 6). The diabetic heart exhibits insulin resistance, resulting in impaired glucose uptake and oxidation (8). This metabolic inflexibility leads to intra-cardiac glucose overload, activating a glucotoxic response that ultimately compromises cardiac function (9). Several cellular pathways have been implicated in this glucotoxic response in the diabetic heart, including activation of oxidative stress, accumulation of advanced glycation end-products (AGEs), increased flux through the polyol pathway, and chronic activation of the hexosamine biosynthetic pathway (HBP) responsible for protein O-GlcNAcylation (10).

To further explore the mechanisms underlying DCM, we and others previously investigated the cardiac phenotype of lipodystrophic and severely insulin-resistant seipin knockout (SKO) mice (11–13). SKO mice exhibit left ventricular hypertrophy and diastolic dysfunction, as evidenced by a reduced early-to-late ventricular filling velocity ratio (E/A ratio) (12), prolonged isovolumetric relaxation time (12, 13), altered myocardial performance, and a modest but significant reduction in ejection fraction. We

previously reported chronic activation of the HBP in SKO mice, and treatment with a sodium–glucose cotransporter-2 (SGLT2) inhibitor reduced cardiac O-GlcNAcylation levels and improved functional parameters. Notably, cardiomyopathy in SKO mice developed in the absence of fibrosis, lipid accumulation, or AGE deposition. These findings suggested that elevated O-GlcNAcylation plays a central role in the cardiac phenotype of SKO mice; however, our earlier work remained correlative and did not directly demonstrate a causal role for the HBP in this context.

The HBP provides N-acetylglucosamine moieties (O-GlcNAc) that are O-linked by the O-GlcNAc transferase (OGT) to serine and threonine residues of proteins, and removed by the O-GlcNAcase (OGA) (14). O-GlcNAcylation regulates the activity and stability of target proteins and has been described across species and organs as part of a cellular stress response (15). Early studies reported chronic activation of the HBP in the hearts of diabetic rodent models, suggesting increased glucose flux through this pathway under hyperglycemic conditions (16–20). Importantly, elevated levels of O-GlcNAcylated proteins have been observed in cardiac biopsies from patients with HF (21). Extensive research has sought to elucidate how chronic O-GlcNAcylation impairs cardiac function. *In vitro*, pharmacological modulation of the HBP revealed that elevated O-GlcNAcylation directly alters excitation–contraction coupling (22). In diabetic rodent hearts, contractile proteins such as myosin heavy chain, actin, and tropomyosin are excessively O-GlcNAcylated, and removing GlcNAc residues with recombinant OGA restores normal contractile properties in cardiac skinned fibers (23). In neonatal rat cardiomyocytes, high-glucose exposure increases mitochondrial protein O-GlcNAcylation and impairs mitochondrial function, whereas OGA restores ATP production (24). Similarly, in the hearts of insulin-resistant rats, several mitochondrial proteins are over-O-GlcNAcylated (25), and increased O-GlcNAcylation of the mitochondrial fission regulator DRP1 is associated with enhanced mitochondrial fragmentation (26).

To establish the causal role of chronic HBP activation in cardiac dysfunction, several studies have manipulated O-GlcNAcylation levels in rodent models of cardiovascular disease. *In vivo*, AAV-mediated overexpression of OGA improved cardiac contractile properties in low-dose streptozotocin (STZ) under high-fat diet diabetic mice (16). More recently, a study demonstrated that cardiac AAV-mediated overexpression of OGT alone is sufficient to induce left ventricular hypertrophy, diastolic dysfunction, and oxidative stress, whereas OGA overexpression attenuates diastolic dysfunction in a mouse model of type 1 diabetes (27). Beyond diabetes, transverse aortic constriction (TAC) is also associated with elevated O-GlcNAc levels, and O-GlcNAcylation of several transcription factors—including NFAT (28), GATA4, and MEF2C (29)— enhances their activity and promotes hypertrophic gene expression. Limiting chronic HBP activation, either by OGA overexpression (30) or through AMPK activation (31), mitigates cardiac hypertrophy in different rodent models.

In the present study, we addressed this question by using AAV-mediated cardiac overexpression of OGA in SKO mice to assess its impact on cardiac function. We further identified the proteins excessively O-GlcNAcylated in SKO hearts and highlighted β-catenin as a major target. Finally, we examined whether β-catenin inhibition could attenuate cardiac dysfunction in SKO mice and blunt the hypertrophic response in isolated cardiomyocytes. Altogether, our work aims to demonstrate the causal role of chronic O-

GlcNAcylation in a mouse model of severe insulin resistance and to uncover the central contribution of β-catenin O-GlcNAc–mediated activation to the associated cardiac phenotype.

METHODS

Animals. SKO mice were generated as previously described (32). For cardiac reversion of over O-GlcNAcylation experiment, at 4 weeks of age, WT mice were injected with AAV9-GFP control virus and SKO mice with either AAV9-GFP or AAV9-hOGA. Viral vectors were from VectorBuilder (VB191112-1784rfv and VB191112-1776gqd), GFP and hOGA expression were driven by the cTnT promoter and were injected in the retro-orbital sinus at the dose of $1.5x10^{12}$ particles per mouse. Echography was performed at 12 weeks of age and mice were sacrificed and organs collected at 14 weeks of age. For β-Catenin inhibition in SKO mice experiment, seven weeks-old WT and SKO mice were daily subcutaneously injected with ICG-001 (Biorbyt - orb1710780–40mg/kg/day) or vehicle (49% Nacl, 49% PEG300, 2% DMSO). Echography was performed at 12 weeks of age and mice were sacrificed and organs collected at 14 weeks of age. For the HFD model of DCM, eight weeks-old male C57Bl/6J mice (Charles River) were fed a high-fat diet (HFD) (60% of calories from fat, D12492 Research diets), or a standard chow diet for 6 months. Echography was performed 10 days before mice sacrifice and organ collection. For the streptozotocin/HFD model of DCM, ten weeks-old male C57Bl/6J mice (Charles River) were injected with low dose of streptozotocin (STZ, i.p., 75mg/kg) and fed a high-fat diet (HFD) (60% of calories from fat, D12492 Research diets), or injected with vehicle and fed a standard chow diet for 4 months. Echography was performed 2 weeks before mice sacrifice and organ collection. All mice had *ad libitum* access to food and water and were housed in the same open mouse facility on a 12/12-h light/dark day/night cycle. Animal care and study protocols were approved by the French Ministry of Education and Research and the ethics committee N°6 in animal experimentation (APAFiS #15323 and #46459) and were in accordance with the EU Directive 2010/63/EU for animal experiments.

Insulin signaling. Twelve-week-old SKO and WT mice were fasted for 2 h, and a single dose of 0.75 UI/kg of human recombinant insulin (Umuline rapide, Eli Lilly, Suresnes, France) was administered by intravenous injection. The mice were killed 5 min after injection, and the hearts were collected and washed in PBS.

Echocardiography. Echocardiographic exams were performed using the Vevo 3100 (Fujifilm VisualSonics) with the MX550D transducer (25–55 MHz). Briefly, mice were anesthesized using isoflurane (induction at 4%, maintain at 2%) for echocardiographic evaluation. Animals were placed in supine position and body temperature was maintained at 37°C, thanks to the termo-regulated platform. The mouse chest was shaved using a chemical hair remover. Echocardiographic acquisition was done according to the current recommendations(33). LV remodeling was characterized on parasternal short-axis view at the mid-ventricular level using M-mode. LV dimensions were measured offline on the VevoLab software (Fujifilm VisualSonics) by experts blinded to mouse genotype, and included left ventricular anterior wall thickness in diastole (LVAWd), left ventricular posterior wall thickness in diastole

(LVPWd), and left ventricular internal dimensions in diastole (LVIDd). LV mass (LVM) was estimated based on these parameters (33). An average from at least 3 different cycles was reported.

Pull-Down of O-GlcNAcylated proteins. Cardiac proteins were extracted with RIPA containing protein inhibition cocktail (Sigma Aldrich) and NButGT (40 µM final). 750 µg of heart proteins were incubated with 40µL of agarose bound wheat germ agglutinin (Vector Laboratories – 2 hours at 4°C on a rotating wheel). After centrifugation (2min, 3000rpm, 4°C), supernatant was discarded, beads were washed 3 times with RIPA, centrifuged again and the resultant pellet containing O-GlcNAcylated proteins was used for western blot.

Western Blots. For western blot analyses, we used phospho-SER473-AKT, pan-AKT, O-GlcNAc (CTD110.6) antibodies from Cell Signaling; β-CATENIN antibody from BD Bioscience; and Tubulin antibody from Sigma Aldrich.

O-GlcNAcylated large scale protein analysis.

1.8 mg of proteins were extracted from hearts of control and SKO mice (n = 8 in each group) in buffer containing Tris 50mM, pH8 ; NaCl, 137mM ; Glycérol 10%, Triton 1%, 10mM of PUGNAc as well as proteases and phosphatases inhibitors (extraction buffer). Lysates were incubated during 2 hours on 125 µL of agarose bound wheat germ agglutinin (WGA, Vector Laboratories – 2 hours at 4°C on a rotating wheel). After centrifugation (2min, 3000rpm, 4°C), supernatant was discarded, beads were washed 3 times with 1 ml of extraction buffer and 2 times with 1 ml of the same buffer containing only 0.1%Triton (washing buffer). O-GlcNAcylated proteins were then eluted with 4 x 0.5ml of elution buffer containing 0.375 M of N-Acetyl glucosamine dissolved in washing buffer. Eluates were concentrated on Centricon (2K) to a volume of 250 µl and diluted to 2.5ml in buffer without Triton and N acetyl-glucosamine that may interfere with the proteomic procedure, and concentrated again to 250 µl.

In parallel, proteins from the same heart samples were extracted in buffer containing 100mM Tris, pH8, 4% SDS for direct label free analysis of the global proteome in each sample. This permitted to normalize for each protein the amount of glycosylated proteins eluted from the WGA to the amount of protein initially present in the heart lysate.

Maxquant software version 1.6.6.0 (Cox. J et al. 2014) was used for the data extraction from the raw MS files of glycosylated proteins eluted from the WGA and of the global proteome together. The databases used were the mouse sequences from the Uniprot database (June 2018) and a list of in-house frequent contaminant sequences. The cleavage specificity was trypsin's with maximum 2 missed cleavages. Carbamidomethylation of cysteines was set as constant modification, whereas acetylation of the protein N terminus, O-GlcNAcylation of Serine and Threonine and oxidation of methionines were set as variable modifications. The false discovery rate was kept below 1% on both peptides and proteins. The normalization was not permitted and "match between runs" (MBR) option was allowed with a match time window of 1 min and an alignment time window of 20 min between global analyses on the one hand and between enrichment analyses on the other.

Perseus software version 1.6.2.3 was used for data analysis from the Protein group files of Maxquant. After eliminating reverse proteins, contaminant proteins and the only identified by site, LFQ intensity data were transformed by Log2. To normalize the amount of glycosylated proteins eluted from the WGA to the amount of protein initially present in the heart lysate, the LFQ value of each protein detected in WGA samples were divided by the LFQ value of the global proteome analysis. A filter was applied to keep only proteins with at least 70% of valid normalized ratio in at least one of the two conditions (SKO or WT). Then, student t.test was calculated between the two conditions and only proteins with a p value < 0.05 were kept. To detect if these significantly different proteins were overglycosylated in SKO or not, a new ratio was calculated by dividing the SKO LFQ value by the WT LFQ value of WGA samples. A threshold of 1.4 (Log2 ratio > 0.5) was set to consider overglycosylation in SKO hearts.

RNA extraction and analysis. RNA from heart was extracted using Trizol and purified using the NucleoSpin RNA kit (Macherey-Nagel). For qPCR, 1 µg RNA was reverse-transcribed using the High-Capacity cDNA Reverse Transcription Kit (Thermo Fisher Scientific). Quantitative PCR was performed using PowerSYBR Green PCR Master Mix on the QuantStudio 5 system (Thermo Fisher Scientific) according to the manufacturer's instructions. Primers sequences are available on request. For 3’seq-RNA profiling, the libraries were prepared from 10 ng of total RNA in 4 µL. The mRNA poly(A) tails were tagged with universal adapters, well-specific barcodes and unique molecular identifiers (UMIs) during template-switching reverse transcriptase. Barcoded cDNAs from multiple samples were then pooled, amplified, and fragmented using a transposon-fragmentation approach that enriches for 3'ends of cDNA: 200 ng of full-length cDNAs was used as input to the Nextera DNA Sample Prep kit (ref FC-121-1030, Illumina). Library size was controlled on a 2200 Tape Station System (Agilent Technologies). A library of 350–800 bp length was run on a NovaSeq6000 using NovaSeq6000 SP reagent 100 cycles (ref #20027464, Illumina) with 17-8-105 cycles reads. Raw fastq pairs matched the following criteria: the 16 bases of the first read correspond to 6 bases for a designed sample-specific barcode and 10 bases for a unique molecular identifier (UMI). The second read (104 bases) corresponds to the captured poly(A) RNA sequence. We performed demultiplexing of these fastq pairs to generate one single-end fastq for each of the 96 samples. These fastq files were then aligned with bwa to the reference mRNA refseq sequences and the mitochondrial genomic sequence, both available from the UCSC download site. Data have been deposited at GEO and are publicly available as of the date of publication. The dataset identifier is GSE334965.

Cell culture:

Primary cultured cardiomyocytes. Isolation, treatment and size measurement of neonatal rat ventricular myocytes (NRVMs) were done as previously shown (31). NRVMs were isolated, cultured under aseptic conditions and plated coverslips coated with gelatin. Prior to treatment, NRVMs were serum-deprived in IMDM medium for 2 hours. For prevention experiments, NRVMs were sco-treated with pro-hypertrophic agents, phenylephrine (PE, 20 µM, #2838 Biotechne) and/or ICG-001 (5 µM, Biorbyt) for 24 hours. For reversibility studies, NRVMs were pre-treated with PE for 24h, followed by ICG-001 treatment for an additional 24 hours. At the end of the treatments, cells were washed twice with ice-cold phosphate-

buffered saline (PBS), fixed with 4% formaldehyde and permeabilised with 0.2% Triton X-100 for 30 min on ice. After fixation, cells were blocked in 1% BSA in PBS for 40 min and incubated for 1 h at room temperature with an anti-α-actinin (1/1000 dilution, #7811 Sigma) primary antibody diluted in blocking solution. Cells were then incubated with an Alexa Fluor 594-conjugated anti-mouse (1/1000 dilution, #A2103 Invitrogen) secondary antibody. Cells were visualized using a Zeiss AxioImager.z1 microscope, and images were captured at ×20 magnification. Cell size (> 100 cells per sample) was measured using ImageJ software.

Isolation, treatment and size measurement of adult rat ventricular myocytes (ARVMs) were performed as previously described (31). Briefly, heart from 250 g male Wistar rats was rapidly excised and retrogradely perfused via the aorta with Ca^{2+}-free Krebs–Henseleit buffer. Enzymatic digestion was performed using buffer supplemented with 0.2 mM Ca^{2+}, 1 mg mL^{-1} type II collagenase and 0.4% (w/v) fatty acid-free BSA, followed by gentle mechanical dissociation. Cardiomyocytes were purified by sedimentation, resuspended in Medium 199 and plated onto laminin-coated dishes. After 1 h, cells were infected with adenoviral particles encoding for GFP (adenoviral control, 30 MOI) or dual aptamer constructs (30 MOI) (34). Briefly, a subset of cells was treated with a linked dual aptamer designed to spatially recruit the OGT enzyme in proximity to the β-catenin protein, thereby promoting its O-GlcNAcylation. In parallel, control cells were incubated with a non-linked dual aptamer, which does not facilitate OGT–β-catenin proximity and therefore does not enhance β-catenin O-GlcNAcylation. 2 hours post-infection, cells were stimulated with the pro-hypertrophic agent, phenylephrine (PE, 100 µM), and the medium was replaced with Medium 199 supplemented with 2 mM carnitine, 5 mM creatine, 5 mM taurine, 10^{-10} M triiodothyronine (T3), 0.2% (w/v) fatty acid-free BSA and antibiotics. After 48 h, cells were washed twice with ice-cold phosphate-buffered saline (PBS) and cell visualized using microscope Olympus IX71, and images were captured at ×10 magnification. Cell size (> 100 cells per sample) was measured using FIJI software.

Respiratory assay. Isolated cardiac mitochondria respiration was assessed with the Seahorse XF96 analyzer according to the manufacturer recommendations (https://www.agilent.com/cs/library/applications/5991-7144EN.pdf). The ventricles were cut into about ten pieces, rinsed with PBS, homogenized using a Potter homogenizer in 1.5 mL of mitochondrial isolation buffer (MIB) and centrifuged (10min, 500g). Supernatant was filtered (100µm) and centrifuged (10min, 10000g). Pellet was washed in MIB, centrifuged again and resuspended in 500µL of mitochondria assay solution (MAS). Protein content was assessed with BCA (BCA protein assay - Thermo Fisher) and mitochondria (1µg of protein content per well) were used for Seahorse coupling assay and electron flow assay. Pyruvate and succinate were used as energy substrates for the coupling assay.

Statistical Analysis. Data are expressed as mean ± SEM. Differential effects were analyzed by analysis of variance or by Student's t-tests. Two-way ANOVA was used where indicated to test for interactions between experimental groups and variables. All analyses were performed using GraphPad Prism. A $p < 0.05$ was considered statistically significant.

RESULTS

Reduction of cardiac O-GlcNAcylation mitigates cardiac hypertrophy and insulin resistance in Seipin KO mice.

We previously showed that cardiac over O-GlcNAcylation was positively associated with cardiac dysfunction in SKO mice (12). To assess the causal role of O-GlcNAcylation excess, we overexpressed human OGA, the enzyme that hydrolyses O-GlcNAc residues, under the control of the cardiac-specific Troponin T promoter in the heart of SKO. We first assessed hOGA overexpression in SKO mice by qPCR (**Fig. 1A**) and then tested the effect on cardiac O-GlcNAcylation levels. hOGA expression decreased the over-O-GlcNAcylation of SKO mice to a level close to that of wild-type (WT) mice (**Fig. 1B**). We next sought to determine the effect of hOGA overexpression on cardiac parameters. Heart somatic index, representing the ratio of heart weight to tibia length, is increased in SKO mice compared with the WT littermates but reduced by OGA overexpression (**Fig. 1C**). Echocardiography analysis confirmed that diastolic left ventricular thickness of anterior (LVAW) and posterior (LVPW) walls and left ventricular mass (LVM) were increased in SKO compared with WT mice, whereas hOGA overexpression normalized it (**Fig. 1D**). Of note, these improvements in hOGA-treated SKO mice were not associated with a reduction of hyperglycemia by hOGA cardiac overexpression (**Supplemental Fig. 1**). We next measured the expression of genes involved in the regulation of cardiac hypertrophy (*Anp*, *ßMhc*/*αMhc* ratio), remodeling (*Ctgf*, *Timp2, Postn*), or failure (*Igfbp5).* Cardiac expression of these genes was increased in SKO versus WT animals, and was reverted in SKO following hOGA expression (**Fig. 1E**). Another key feature of SKO failing heart is insulin-resistance (12). We analyzed the cardiac insulin response in SKO mice expressing either hOGA or GFP by measuring ser-473 AKT phosphorylation levels and found a 70% increase in hOGA-expressing animals, suggesting improved insulin sensitivity (**Fig. 1F**). Altogether, these results show that in SKO mice, hOGA overexpression in the heart corrects cardiac hypertrophy and insulin resistance.

Identification of over O-GlcNAcylated proteins in SKO mice

To understand how chronic O-GlcNAcylation affects cardiac properties, we performed proteomics analysis of total and O-GlcNAcylated proteins obtained by agglutinin-driven pulldown (**Fig. 2A**). We identified 40 proteins with modified O-GlcNAcylated/total ratio between genotypes, 21 of which are over O-GlcNAcylated in SKO compared to WT hearts (**Table 1**). Several of these over O-GlcNAcylated proteins are involved in mitochondria homeostasis (6), extra-cellular matrix (4), cytoskeleton (2), cellular junction (1), transmembrane proteins, and in other cellular functions. In parallel, we performed RNA sequencing, and gene ontology analysis revealed that the modulated pathways are almost exclusively related to mitochondrial functions (**Fig. 2B**). Thus, we assessed the respiratory capacity of mitochondria isolated from WT and SKO mice expressing either GFP or hOGA. Compared to WT, SKO cardiac mitochondria exhibited higher oxygen consumption under basal conditions (state II), during ADP stimulation (state III), and when succinate was used as the primary substrate (**Supplemental Fig. 2A-D**). Consistently, the

activities of complexes I and II were also elevated in SKO mice (**Supplemental Fig. 2E**). However, hOGA overexpression in SKO mice did not alter these mitochondrial parameters, indicating that the hOGA-mediated reduction in O-GlcNAcylation improves cardiac function in SKO mice independently of changes in mitochondrial respiration.

β **-Catenin activity is increased in SKO hearts and reverted by hOGA overexpression**

Different proteins linked to cardiac dysfunction can be found in our analysis (**Table 1**). Among them, β-catenin appeared like a promising candidate. Indeed, it has been shown that O-GlcNAcylation stabilizes β-catenin and thereby increases its transcriptional activity (35), whereas cardiac deletion of β-Catenin decreases TAC-related hypertrophy (36). We therefore postulated that elevated O-GlcNAcylation of β-catenin (**Table 1**) enhances its transcriptional activity in SKO hearts. We measured the mRNA levels of Wnt/β-catenin pathway genes (*Myc*, *Igfbp5*, *Cnn1*, *Tbx5*, *Jun*, *Fos, Snail1*,*Dkk3*, *Wnt2*, and *Srtfp1*), and observed an increase in SKO versus WT hearts (**Fig. 3**). In SKO hOGA hearts, their levels are either lower compared to SKO hearts (*Myc*, *Igfbp5*, *Cnn1*, *Snail1*, *Dkk3*, *Wnt2*) or not increased when compared to the WT group (*Tbx5*, *Jun*, *Fos*, *Sfrp1* - **Fig. 3**). These findings indicate that β-catenin activity is elevated in SKO hearts and attenuated by hOGA overexpression.

β **-Catenin inhibition in SKO mice prevents cardiac hypertrophy.**

To determine whether β-Catenin overactivation is implicated in the cardiac defects of SKO mice, we treated WT and SKO mice with ICG-001, a β-catenin inhibitor (37). After 7 weeks of treatment, we first assessed ICG-001 efficiency on β-catenin transcriptional activity. In SKO mice, ICG-001 reduces the expression of β-catenin target genes (*Cnn1*, *Tbx5*, *Dkk3*, *Wnt2*, *Wnt4*), without affecting their basal expression in WT mice (**Fig. 4A**). As shown in Fig. 1, cardiac parameters—including the heart-to-body weight ratio, left ventricular mass, and LVAW and LVPW thickness—were all increased in SKO compared with WT mice. Importantly, ICG-001 treatment normalized these parameters in SKO mice, while having no effect in WT animals. (**Fig. 4B,C**). Moreover, in SKO hearts, ICG-001 prevented or reduced the overexpression of genes involved in heart remodelling or failure (*Igfbp5*, *Ctgf* and *Postn*) without affecting *Anp* expression or the b/a *Mhc* ratio (**Fig. 4D**). These ICG-001 experiments highly suggests that β-catenin inhibition is sufficient to prevent cardiac hypertrophy in SKO mice.

Increased O-GlcNAcylation levels of β**-catenin, a hallmark of various murine models of DCM**

To extend the role of β-Catenin O-GlcNAcylation and its overactivation in DCM development, we used two more common murine models. In 6 months HFD fed mice (**Fig. 5A-D**) and in low-dose STZ-injected mice followed by 4 months of HFD feeding (**Fig. 5E-H**), we observed a cardiac hypertrophy highlighted by either an increase of heart weight or of the left ventricular free wall compared with the control groups (**Fig. 5A,E**). In both diabetes models, cardiac hypertrophy was associated with increased cardiac O-GlcNAcylation (**Fig. 5B,F**), with a specific increase in the O-GlcNAcylation of cardiac β-catenin. In hearts of HFD fed mice, *Myc* and *Igfbp5* mRNA levels were increased, whereas in STZ-injected mice only *Myc* expression was induced **(Fig. 5D,H)**.

β -catenin activity and O-GlcNAcylation levels control cardiomyocyte hypertrophy in vitro

β-catenin has been previously shown to participate in cardiac hypertrophy development (38). Furthermore, O-GlcNAcylomic analyses of a pressure overload-induced cardiac hypertrophy mouse model revealed a similar increase in the O-GlcNAcylation level of β-catenin (personal communication of L. Bertrand). To gain insight into the mechanisms at play, we next used primary cultured cardiomyocyte models. First, NRVMs were treated with the pro-hypertrophic agent PE. As previously shown (31), PE promoted NRVM hypertrophy, highlighted by α-actinin immunolabelling (**Fig. 6A**). This 35% increase in cardiomyocyte area was strikingly prevented by ICG-001 co-treatment, whereas ICG-001 alone had no impact on cardiomyocyte size (**Fig. 6A**). In another experimental setup, NRVMs were first treated with PE to induce hypertrophy, and ICG-001 was added 24 hours later to assess its ability to reverse established hypertrophy. PE-treated cardiomyocytes displayed a 50% increase in cell size after 48 hours compared with control conditions, and β-catenin inhibition blunted this effect, abolishing the statistical significance relative to control (**Fig. 6B,C**). We then questioned whether specific over O-GlcNAcylation of β-catenin is sufficient to induce hypertrophy. We took advantage of the recently developed dual aptamer, which promotes the interaction between OGT and β-catenin, thereby inducing the specific O-GlcNAcylation of β-catenin (34). This dual aptamer was cloned into an adenoviral expression system and overexpressed in cultured ARVMs. We measured cardiomyocyte area and found that overexpression of the aptamer induced a 20% increase compared with control or non-linked control aptamer (**Fig. 6D**). Notably, the pro-hypertrophic effect of the aptamer was similar to that observed with PE treatment. These data demonstrate that excessive O-GlcNAcylation of β-catenin alone is sufficient to promote cardiomyocyte hypertrophy.

DISCUSSION

In this study, we investigated the causal role of O-GlcNAcylation in DCM observed in SKO mice, a model of generalized lipodystrophy and severe insulin resistance. Using AAV-mediated cardiac overexpression of OGA, we successfully corrected both cardiac hypertrophy and insulin resistance in SKO hearts. Proteomic analyses revealed that β-catenin is highly O-GlcNAcylated in SKO heart lysates, accompanied by increased expression of its transcriptional targets. Notably, elevated β-catenin O-GlcNAcylation was also detected in two additional models of T2D. Importantly, pharmacological inhibition of β-catenin attenuated cardiac hypertrophy both in SKO mice and in isolated cardiomyocytes. Finally, β-catenin O-GlcNAcylation alone was sufficient to induce cardiomyocyte hypertrophy *in vitro*. Collectively, our findings demonstrate that chronic O-GlcNAcylation is a causal driver of cardiac hypertrophy in SKO mice and suggest that O-GlcNAc–mediated activation of β-catenin plays a central role in this phenotype.

The first key question of this work was whether limiting chronic activation of protein O-GlcNAcylation could mitigate DCM features in SKO mice. By overexpressing OGA, we reverted the main cardiac alterations observed in SKO animals—namely hypertrophy and insulin resistance. Since cardiac hypertrophy in SKO mice was not associated with lipotoxicity, advanced glycation end-products, or oxidative stress, this result strongly supports the notion that elevated O-GlcNAcylation plays a central

role in the pathophysiology of DCM in this model. The attenuation of hypertrophy is consistent with previous studies performed in STZ-treated mice (27) (a model of type 1 diabetes) and in low-STZ/HFD mice (a model of type 2 diabetes–associated DCM) (16). However, our data further demonstrate that normalizing protein O-GlcNAcylation level by OGA overexpression improves cardiac insulin sensitivity in SKO mice.

We next investigated how chronic activation of protein O-GlcNAcylation contributes to cardiac phenotype. Proteomic analysis of SKO hearts revealed 28 over-O-GlcNAcylated proteins, including 6 mitochondrial proteins, in agreement with previous reports showing increased O-GlcNAcylation of mitochondrial proteins in rodent models of diabetes (25, 39). Moreover, transcriptomic analyses identified mitochondria as a major cellular compartment affected in SKO hearts. To assess the functional relevance of these findings, we measured mitochondrial oxygen consumption in isolated cardiac mitochondria. We found that mitochondrial activity and oxygen consumption were increased in SKO hearts but not normalized by OGA overexpression. This enhanced mitochondrial activity is consistent with previous studies showing increased mitochondrial respiration in the context of mitochondrial over-o-GlcNAcylation (40) and increased fatty acid oxidation in SKO hearts that was corrected by the inhibition of the adipose tissue triglyceride lipase (ATGL) (11). In our study, the improvement of LVH by OGA overexpression occurred independently of mitochondrial activity normalization. However, we cannot exclude a contribution of mitochondrial O-GlcNAcylation to the pathophysiology of SKO hearts, as the lack of effect on mitochondrial respiration may reflect a technical limitation. Indeed, mitochondria O-GlcNAcylation is driven by specific OGT/OGA/UDP-GlcNAc transport (39). The lack of mitochondrial response to human OGA overexpression that we observed, could be due to the ineffectiveness of our strategy to target mitochondrial O-GlcNAcylation. Indeed, in the present work, we have overexpressed the full-length isoform of OGA (L-OGA). However, it has been shown recently that it is the short splice variant of OGA (S-OGA) that is preferentially addressed to the mitochondria (41). Optimization of OGA-driven O-GlcNAcylation reduction to include mitochondrial proteins would be thus of interest to maximize therapeutic strategies of O-GlcNAc modulation. Nevertheless, despite the absence of mitochondrial rescue, OGA overexpression effectively protected SKO hearts from hypertrophy, suggesting that mitochondrial-independent mechanisms contribute at least partially to DCM in this model.

The most striking consequence of OGA overexpression was the almost complete reversion of cardiac hypertrophy. We identified β-catenin as being over O-GlcNAcylated in SKO hearts compared with WT ones. Consistent with recent reports showing that β-catenin O-GlcNAcylation increases its stability and transcriptional activity (34, 35), we observed upregulation of several β-catenin target genes, supporting its activation by elevated O-GlcNAcylation in SKO mice. β-catenin activation has also been reported in STZ-treated models of diabetes (42) (43), and both genetic (36) and pharmacological inhibition of β-catenin have been shown to mitigate cardiac hypertrophy in pressure overload (TAC) mice (44). In particular, the β-catenin inhibitor ICG-001, which we also used in SKO mice, efficiently reverted the hypertrophic phenotype (44). Using isolated cardiomyocytes, we further demonstrated that β-catenin inhibition limits PE-induced hypertrophy, indicating a cell-autonomous mechanism. To directly link β-

catenin O-GlcNAcylation to hypertrophy, we used an aptamer that enhances β-catenin–OGT interaction, thereby specifically increasing β-catenin O-GlcNAcylation. This was sufficient to promote cardiomyocyte hypertrophy. Beyond the specificity of the lipodystrophic SKO mice, we finally showed that over-O-GlcNAcylation of cardiac β-Catenin is associated with heart hypertrophy in two other models of DCM, proving the "universality" of β-Catenin over-O-GlcNAcylation in DCM. Finally, our findings align with current translational efforts targeting β-catenin, as multiple clinical trials are actively evaluating pharmacological approaches to modulate the Wnt/β-catenin signaling pathway as a potential therapeutic strategy for cardiovascular diseases (45)

Altogether, our results identify O-GlcNAcylation—and specifically β-catenin O-GlcNAcylation—as a key driver of cardiac hypertrophy in SKO mice. Therefore, the β-Catenin over-O-GlcNAcylation could be a clinically interesting target for the treatment of DCM as well as other pathologies involving heart hypertrophy.

Declarations

Ethics declaration

All animal procedures were approved by the French Ministry of Higher Education and Research and the Animal Ethics Committee No. 6 (APAFiS #15323 and #46459), and were conducted in accordance with the European Union Directive 2010/63/EU on the protection of animals used for scientific purposes.

Consent for publication:

All the authors consent the publication of this article

Funding :

This study has been granted from la fondation pour la recherche médicale (FRM, appel d'offre Maladies Cardiovasculaire), la Fondation de France (FDF), et l'Association des jeunes diabétiques (AJD)

Author Contribution

SD, NF, LG, MJ, TI, LB and XP designed the experiments, performed them, analyzed the data and wrote the manuscript. RC, PA, GT, RS, AB, VS, SF, GC, TS, and MC performed experiments. DM, BS, CLM, BC and SH contributed to study design and manuscript writing. All authors reviewed the manuscript.

Acknowledgement

We are most grateful to the Genomics Core Facility GenoA, member of Biogenouest and France Genomique and to the Bioinformatics Core Facility BiRD, member of Biogenouest and Institut Français

de Bioinformatique (IFB) (ANR-11-INBS-0013) for the use of their resources and their technical support. The proteomic analysis has been performed on the Proteom'IC facilty, Université Paris Cité, CNRS, INSERM, Institut Cochin F-75014 PARIS, France. We thank Marjorie Leduc and Cédric Broussard for proteomic experiments. The Orbitrap Fusion mass spectrometer was acquired with funds from the FEDER through the "Operational Programme for Competitiveness Factors and employment 2007-2013", and from the "Cancéropôle Ile-de-France "

Data Availability

Proteomic (PXD079003) and transcriptomic (GSE334965) data are available. All raw data and biological materials are available upon reasonable request.

References

1. McMurray JJV, Solomon SD, Inzucchi SE, Kober L, Kosiborod MN, Martinez FA, et al. Dapagliflozin in Patients with Heart Failure and Reduced Ejection Fraction. N Engl J Med. 2019;381(21):1995–2008.
2. Nichols GA, Gullion CM, Koro CE, Ephross SA, Brown JB. The incidence of congestive heart failure in type 2 diabetes: an update. Diabetes Care. 2004;27(8):1879–84.
3. Nichols GA, Hillier TA, Erbey JR, Brown JB. Congestive heart failure in type 2 diabetes: prevalence, incidence, and risk factors. Diabetes Care. 2001;24(9):1614–9.
4. Rubler S, Dlugash J, Yuceoglu YZ, Kumral T, Branwood AW, Grishman A. New type of cardiomyopathy associated with diabetic glomerulosclerosis. Am J Cardiol. 1972;30(6):595–602.
5. Taegtmeyer H, McNulty P, Young ME. Adaptation and maladaptation of the heart in diabetes: Part I: general concepts. Circulation. 2002;105(14):1727–33.
6. Young ME, McNulty P, Taegtmeyer H. Adaptation and maladaptation of the heart in diabetes: Part II: potential mechanisms. Circulation. 2002;105(15):1861–70.
7. Iribarren C, Karter AJ, Go AS, Ferrara A, Liu JY, Sidney S, et al. Glycemic control and heart failure among adult patients with diabetes. Circulation. 2001;103(22):2668–73.
8. Bertrand L, Horman S, Beauloye C, Vanoverschelde J-L. Insulin signalling in the heart. Cardiovasc Res. 2008;79(2):238–48.
9. Cai L, Li W, Wang G, Guo L, Jiang Y, Kang YJ. Hyperglycemia-induced apoptosis in mouse myocardium: mitochondrial cytochrome C-mediated caspase-3 activation pathway. Diabetes. 2002;51(6):1938–48.
10. Salvatore T, Pafundi PC, Galiero R, Albanese G, Di Martino A, Caturano A, et al. The Diabetic Cardiomyopathy: The Contributing Pathophysiological Mechanisms. Front Med (Lausanne). 2021;8:695792.
11. Zhou H, Lei X, Yan Y, Lydic T, Li J, Weintraub NL et al. Targeting ATGL to rescue BSCL2 lipodystrophy and its associated cardiomyopathy. JCI Insight. 2019;5.

12. Joubert M, Jagu B, Montaigne D, Marechal X, Tesse A, Ayer A, et al. The Sodium-Glucose Cotransporter 2 Inhibitor Dapagliflozin Prevents Cardiomyopathy in a Diabetic Lipodystrophic Mouse Model. Diabetes. 2017;66(4):1030–40.
13. Bai B, Yang W, Fu Y, Foon HL, Tay WT, Yang K, et al. Seipin Knockout Mice Develop Heart Failure With Preserved Ejection Fraction. JACC Basic Transl Sci. 2019;4(8):924–37.
14. Chatham JC, Marchase RB. The role of protein O-linked beta-N-acetylglucosamine in mediating cardiac stress responses. Biochim Biophys Acta. 2010;1800(2):57–66.
15. Dassanayaka S, Jones SP. O-GlcNAc and the cardiovascular system. Pharmacol Ther. 2014;142(1):62–71.
16. Hu Y, Belke D, Suarez J, Swanson E, Clark R, Hoshijima M, et al. Adenovirus-mediated overexpression of O-GlcNAcase improves contractile function in the diabetic heart. Circ Res. 2005;96(9):1006–13.
17. Fülöp N, Mason MM, Dutta K, Wang P, Davidoff AJ, Marchase RB, et al. Impact of Type 2 diabetes and aging on cardiomyocyte function and O-linked N-acetylglucosamine levels in the heart. Am J Physiol Cell Physiol. 2007;292(4):C1370–8.
18. Fricovsky ES, Suarez J, Ihm S-H, Scott BT, Suarez-Ramirez JA, Banerjee I, et al. Excess protein O-GlcNAcylation and the progression of diabetic cardiomyopathy. Am J Physiol Regul Integr Comp Physiol. 2012;303(7):R689–99.
19. Medford HM, Chatham JC, Marsh SA. Chronic ingestion of a Western diet increases O-linked-beta-N-acetylglucosamine (O-GlcNAc) protein modification in the rat heart. Life Sci. 2012;90(23–24):883–8.
20. Marsh SA, Dell'Italia LJ, Chatham JC. Activation of the hexosamine biosynthesis pathway and protein O-GlcNAcylation modulate hypertrophic and cell signaling pathways in cardiomyocytes from diabetic mice. Amino Acids. 2011;40(3):819–28.
21. Lunde IG, Aronsen JM, Kvaloy H, Qvigstad E, Sjaastad I, Tonnessen T, et al. Cardiac O-GlcNAc signaling is increased in hypertrophy and heart failure. Physiol Genomics. 2012;44(2):162–72.
22. Ng YH, Okolo CA, Erickson JR, Baldi JC, Jones PP. Protein O-GlcNAcylation in the heart. Acta Physiol (Oxf). 2021;233(1):e13696.
23. Ramirez-Correa GA, Jin W, Wang Z, Zhong X, Gao WD, Dias WB, et al. O-linked GlcNAc modification of cardiac myofilament proteins: a novel regulator of myocardial contractile function. Circ Res. 2008;103(12):1354–8.
24. Hu Y, Suarez J, Fricovsky E, Wang H, Scott BT, Trauger SA, et al. Increased enzymatic O-GlcNAcylation of mitochondrial proteins impairs mitochondrial function in cardiac myocytes exposed to high glucose. J Biol Chem. 2009;284(1):547–55.
25. Johnsen VL, Belke DD, Hughey CC, Hittel DS, Hepple RT, Koch LG, et al. Enhanced cardiac protein glycosylation (O-GlcNAc) of selected mitochondrial proteins in rats artificially selected for low running capacity. Physiol Genomics. 2013;45(1):17–25.
26. Gawlowski T, Suarez J, Scott B, Torres-Gonzalez M, Wang H, Schwappacher R, et al. Modulation of dynamin-related protein 1 (DRP1) function by increased O-linked-β-N-acetylglucosamine modification (O-GlcNAc) in cardiac myocytes. J Biol Chem. 2012;287(35):30024–34.

27. Prakoso D, Lim SY, Erickson JR, Wallace RS, Lees JG, Tate M, et al. Fine-tuning the cardiac O-GlcNAcylation regulatory enzymes governs the functional and structural phenotype of the diabetic heart. Cardiovasc Res. 2022;118(1):212–25.
28. Facundo HT, Brainard RE, Watson LJ, Ngoh GA, Hamid T, Prabhu SD, et al. O-GlcNAc signaling is essential for NFAT-mediated transcriptional reprogramming during cardiomyocyte hypertrophy. Am J Physiol Heart Circ Physiol. 2012;302(10):H2122–30.
29. Cannon MV, Silljé HHW, Sijbesma JWA, Vreeswijk-Baudoin I, Ciapaite J, van der Sluis B, et al. Cardiac LXRα protects against pathological cardiac hypertrophy and dysfunction by enhancing glucose uptake and utilization. EMBO Mol Med. 2015;7(9):1229–43.
30. Umapathi P, Mesubi OO, Banerjee PS, Abrol N, Wang Q, Luczak ED, et al. Excessive O-GlcNAcylation Causes Heart Failure and Sudden Death. Circulation. 2021;143(17):1687–703.
31. Gelinas R, Mailleux F, Dontaine J, Bultot L, Demeulder B, Ginion A, et al. AMPK activation counteracts cardiac hypertrophy by reducing O-GlcNAcylation. Nat Commun. 2018;9(1):374.
32. Prieur X, Dollet L, Takahashi M, Nemani M, Pillot B, Le May C, et al. Thiazolidinediones partially reverse the metabolic disturbances observed in Bscl2/seipin-deficient mice. Diabetologia. 2013;56(8):1813–25.
33. Zacchigna S, Paldino A, Falcao-Pires I, Daskalopoulos EP, Dal Ferro M, Vodret S, et al. Towards standardization of echocardiography for the evaluation of left ventricular function in adult rodents: a position paper of the ESC Working Group on Myocardial Function. Cardiovasc Res. 2021;117(1):43–59.
34. Zhu Y, Hart GW. Dual-specificity RNA aptamers enable manipulation of target-specific O-GlcNAcylation and unveil functions of O-GlcNAc on beta-catenin. Cell. 2023;186(2):428–45. e27.
35. Olivier-Van Stichelen S, Dehennaut V, Buzy A, Zachayus JL, Guinez C, Mir AM, et al. O-GlcNAcylation stabilizes beta-catenin through direct competition with phosphorylation at threonine 41. FASEB J. 2014;28(8):3325–38.
36. Chen X, Shevtsov SP, Hsich E, Cui L, Haq S, Aronovitz M, et al. The beta-catenin/T-cell factor/lymphocyte enhancer factor signaling pathway is required for normal and stress-induced cardiac hypertrophy. Mol Cell Biol. 2006;26(12):4462–73.
37. Emami KH, Nguyen C, Ma H, Kim DH, Jeong KW, Eguchi M, et al. A small molecule inhibitor of beta-catenin/CREB-binding protein transcription [corrected]. Proc Natl Acad Sci U S A. 2004;101(34):12682–7.
38. Zhao Y, Wang C, Wang C, Hong X, Miao J, Liao Y, et al. An essential role for Wnt/beta-catenin signaling in mediating hypertensive heart disease. Sci Rep. 2018;8(1):8996.
39. Banerjee PS, Ma J, Hart GW. Diabetes-associated dysregulation of O-GlcNAcylation in rat cardiac mitochondria. Proc Natl Acad Sci U S A. 2015;112(19):6050–5.
40. Dontaine J, Bouali A, Daussin F, Bultot L, Vertommen D, Martin M, et al. The intra-mitochondrial O-GlcNAcylation system rapidly modulates OXPHOS function and ROS release in the heart. Commun Biol. 2022;5(1):349.

41. Pagesy P, Bouaboud A, Feng Z, Hulin P, Issad T. Short O-GlcNAcase Is Targeted to the Mitochondria and Regulates Mitochondrial Reactive Oxygen Species Level. Cells. 2022;11(11).
42. Xi XH, Wang Y, Li J, Wang FW, Tian GH, Yin MS, et al. Activation of Wnt/beta-catenin/GSK3beta signaling during the development of diabetic cardiomyopathy. Cardiovasc Pathol. 2015;24(3):179–86.
43. Chen X, Li Y, Yuan X, Yuan W, Li C, Zeng Y, et al. Methazolamide Attenuates the Development of Diabetic Cardiomyopathy by Promoting beta-Catenin Degradation in Type 1 Diabetic Mice. Diabetes. 2022;71(4):795–811.
44. Methatham T, Tomida S, Kimura N, Imai Y, Aizawa K. Inhibition of the canonical Wnt signaling pathway by a beta-catenin/CBP inhibitor prevents heart failure by ameliorating cardiac hypertrophy and fibrosis. Sci Rep. 2021;11(1):14886.
45. Azhdari M, Zur Hausen A. Wnt/beta-catenin and notch signaling pathways in cardiovascular disease: Mechanisms and therapeutics approaches. Pharmacol Res. 2025;211:107565.

Figures

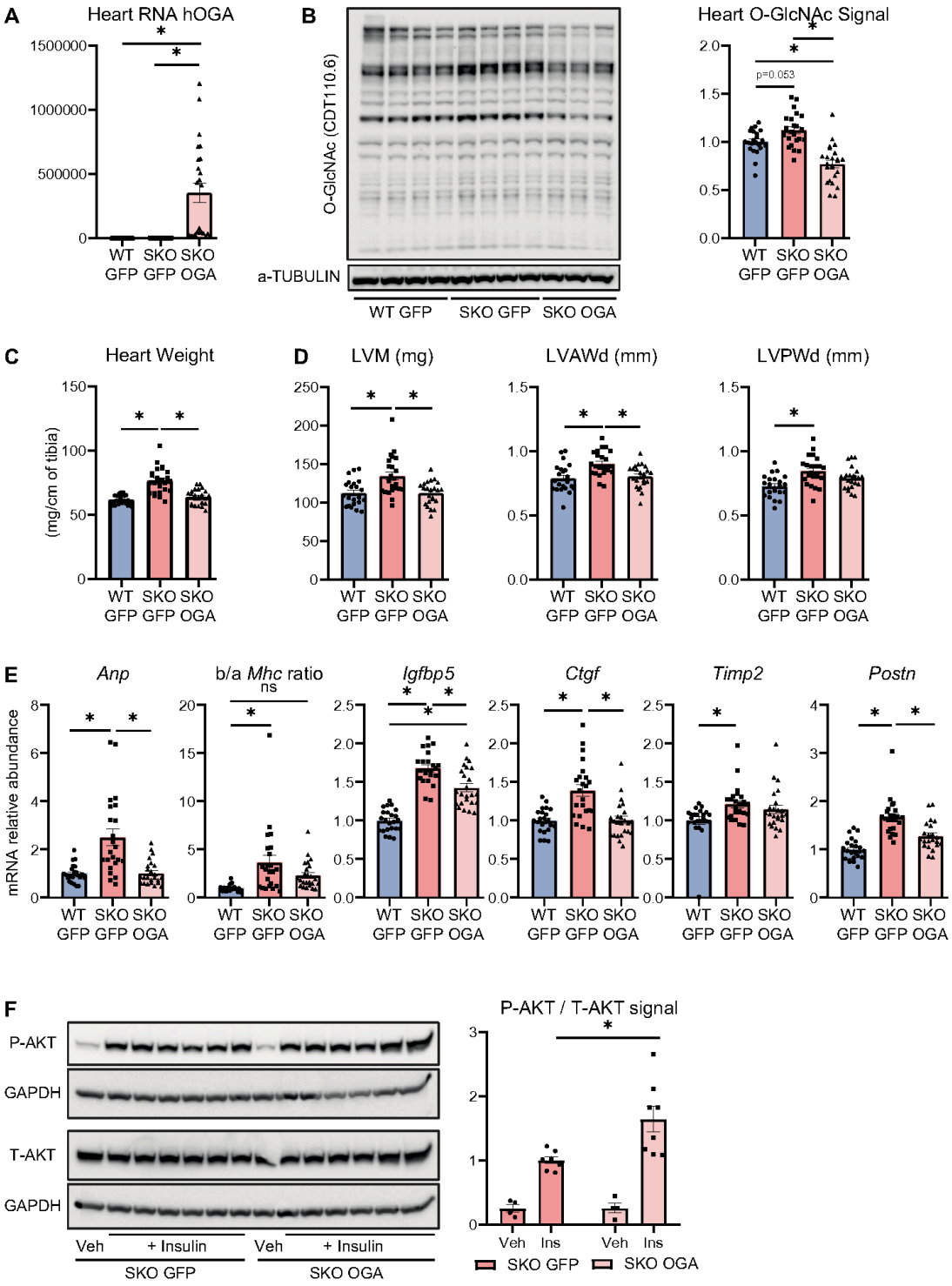


Figure 1

OGA cardiac overexpression reduces heart hypertrophy and ameliorates insulin sensitivity in SKO mice. (A) Cardiac human *OGA* mRNA levels, **(B)** representative western blot and signal quantification of cardiac protein O-GlcNAcylation levels, **(C)** heart somatic index (percentage of heart weight (g) over tibia length (cm)) and **(D)** left ventricular mass (LVM), left ventricular anterior (LVAW) and posterior wall (LVPW) thickness were assessed by echocardiography. **(E)** cardiac *Anp*, ß/a*Mhc* ratio, *Igfbp5*, *Ctgf*, *Timp2*

and *Postn* mRNA levels assessed by qPCR in wild-type (WT) and SKO mice overexpressing either GFP or hOGA in the heart, n=23-24 mice per group. **(F)** Representative western blot and quantification of phosphorylated and total AKT signal measured in the heart of SKO mice overexpressing either GFP or hOGA in the heart and stimulated (n=8 mice per condition) or not (n=4 mice per condition) with insulin. Data are the mean ± SEM. * Significant difference between groups.

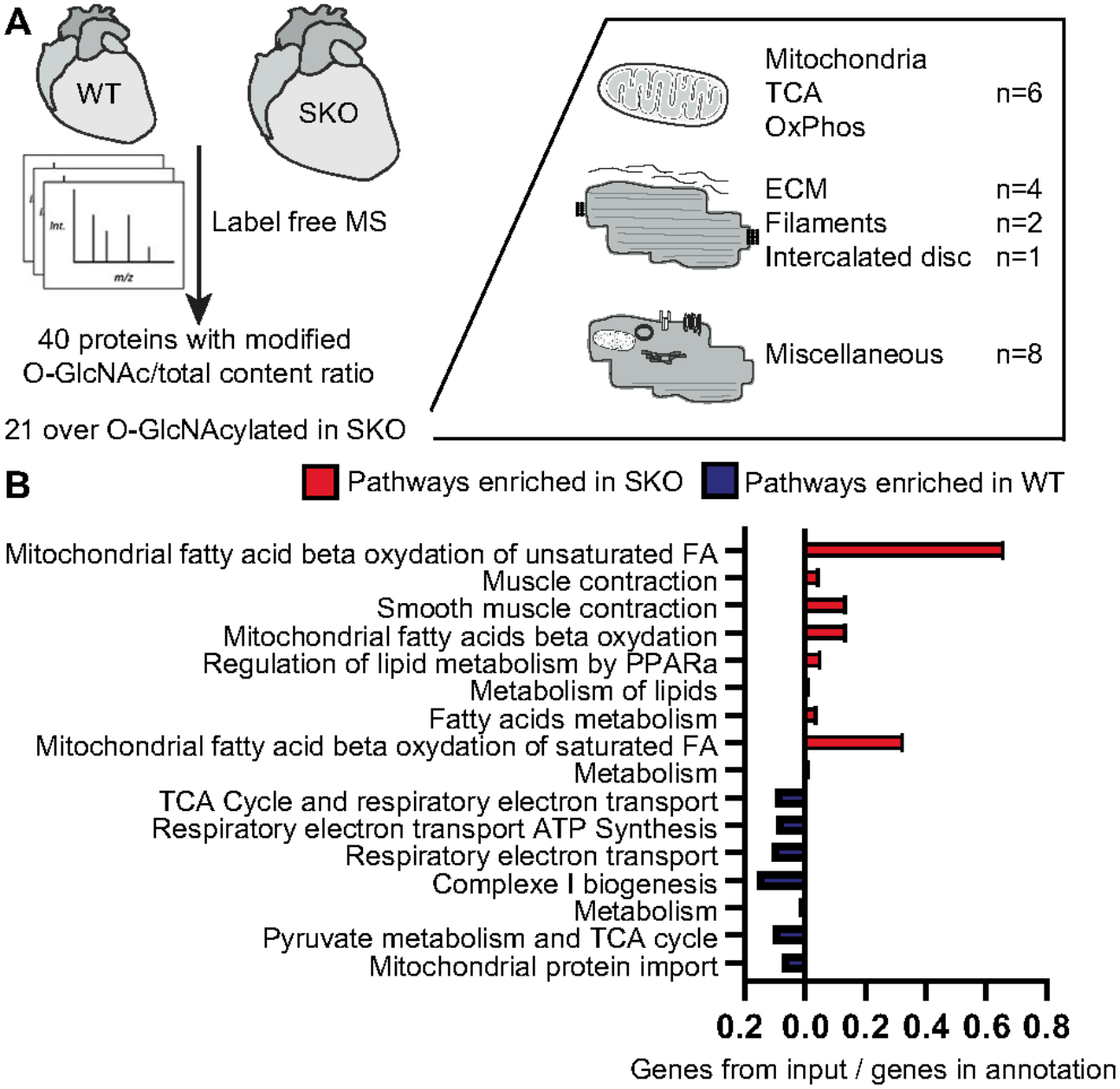


Figure 2

Proteomic and transcriptomic analysis of SKO hearts. (A) Schematic diagram of the strategy used to identify differentially O-GlcNAcylated proteins in the hearts of WT and SKO mice and classification of the over O-GlcNAcylated proteins according to their cellular function (n=8 mice per group). **(B)** Enrichment pathway analysis performed on cardiac transcriptomic data of WT and SKO mice (n=7-8 mice per group).

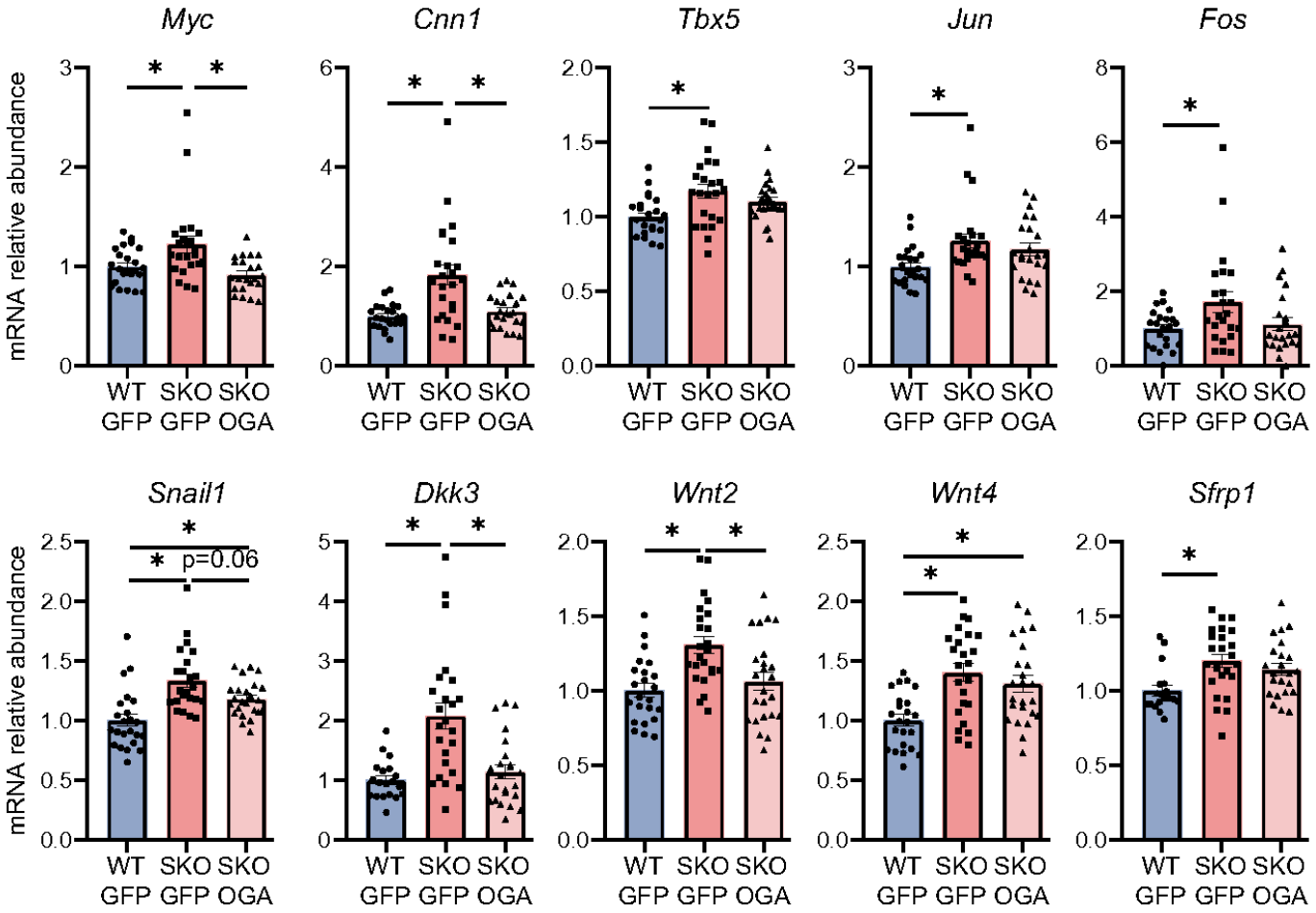


Figure 3

OGA overexpression prevents β-catenin target genes upregulation. *Myc*, *Cnn1*, *Tbx5*, *Jun*, *Fos*, *Snail1*, *Dkk3*, *Wnt2*, *Wnt4* and *Sfrp1* mRNA levels assessed by qPCR in the heart of wild-type (WT) and SKO mice overexpressing either GFP or hOGA in the heart, n=23-24 mice per group. Data are the mean ± SEM. * Significant difference between groups.

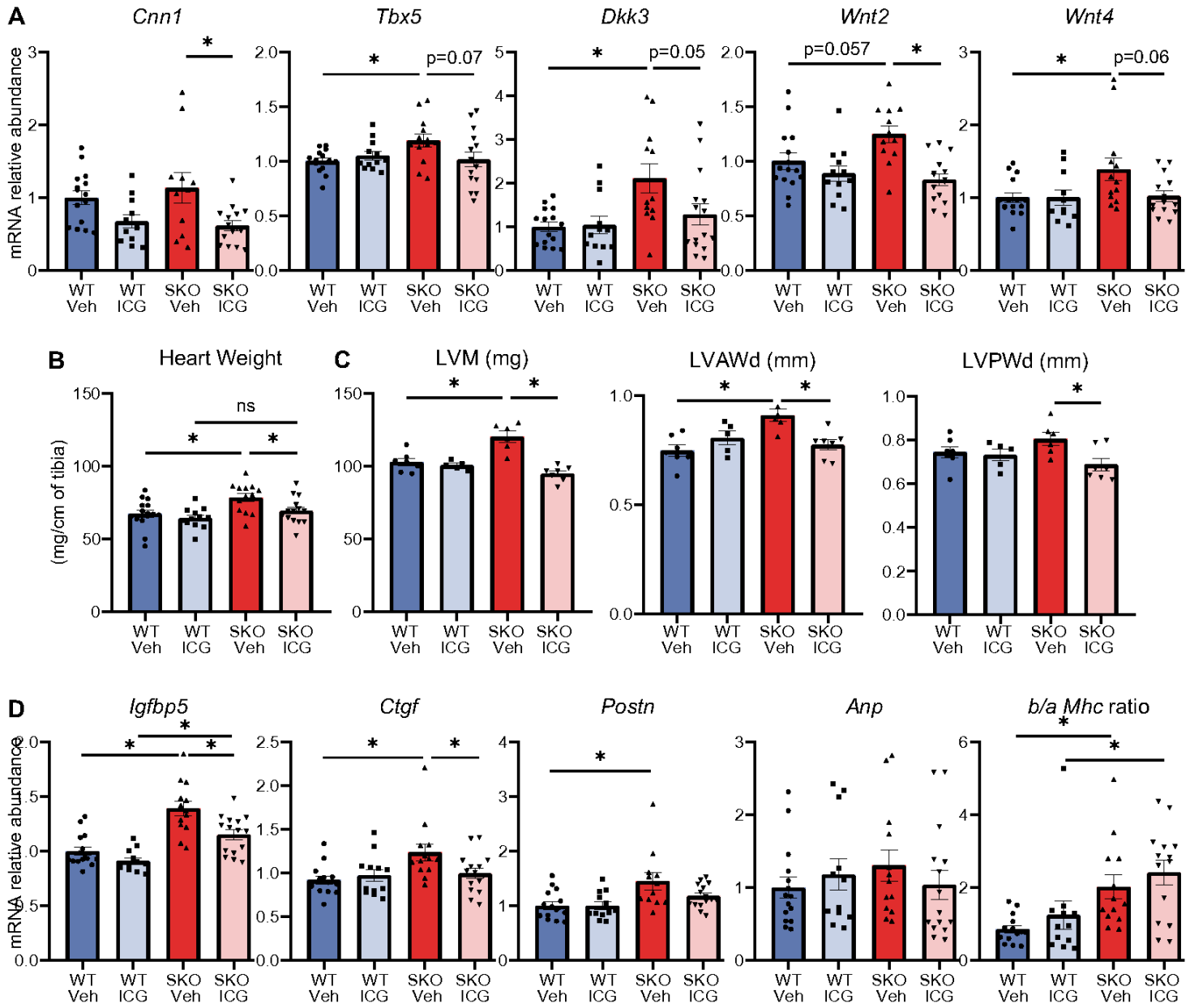


Figure 4

β-catenin pharmacological inhibition mitigates heart hypertrophy in SKO mice. (A) Cardiac *Cnn1*, *Tbx5*, *Dkk3*, *Wnt2* and *Wnt4* mRNA levels assessed by qPCR, **(B)** heart somatic index (percentage of heart weight (g) over body weight (g)) and **(C)** left ventricular mass (LVM), left ventricular anterior (LVAW) and posterior wall (LVPW) thickness assessed by echocardiography, and **(D)** cardiac *Igfbp5*, *Ctgf*, *Postn*, *Anp and* ß/a*Mhc* mRNA levels assessed by qPCR in wild-type (WT) and SKO mice treated or not with ICG-001, n=13-15 mice per group. Data are the mean ± SEM. * Significant difference between groups.

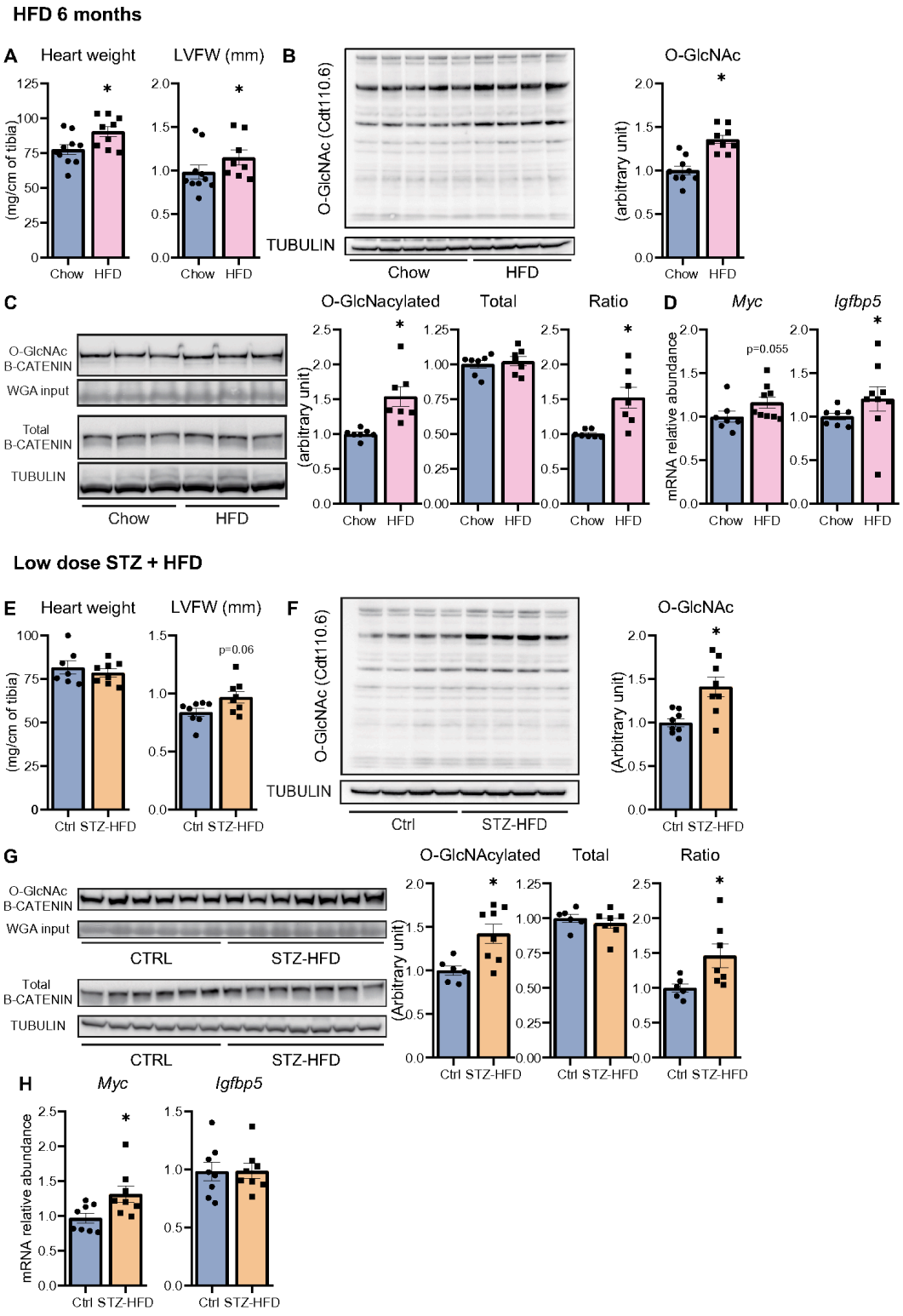


Figure 5

Cardiac β-catenin is over O-GlcNAcylated in different murine models of T2D. (A) Heart somatic index and left ventricular mass (LVM), representative western blot and signal quantification of cardiac **(B)** O-GlcNAcylation levels and **(C)**O-GlcNacylated and total β-catenin content, **(D)** cardiac *Myc* and *Igfbp5*mRNA levels assessed by qPCR in chow- and HFD-fed mice, n=8-9 mice per group. **(E-H)**Same

parameters as in (A-D) but evaluated in control and in mice injected with low doses of streptozotocin and fed a HFD, n=8 mice per group. Data are the mean ± SEM. * Significant difference between groups.

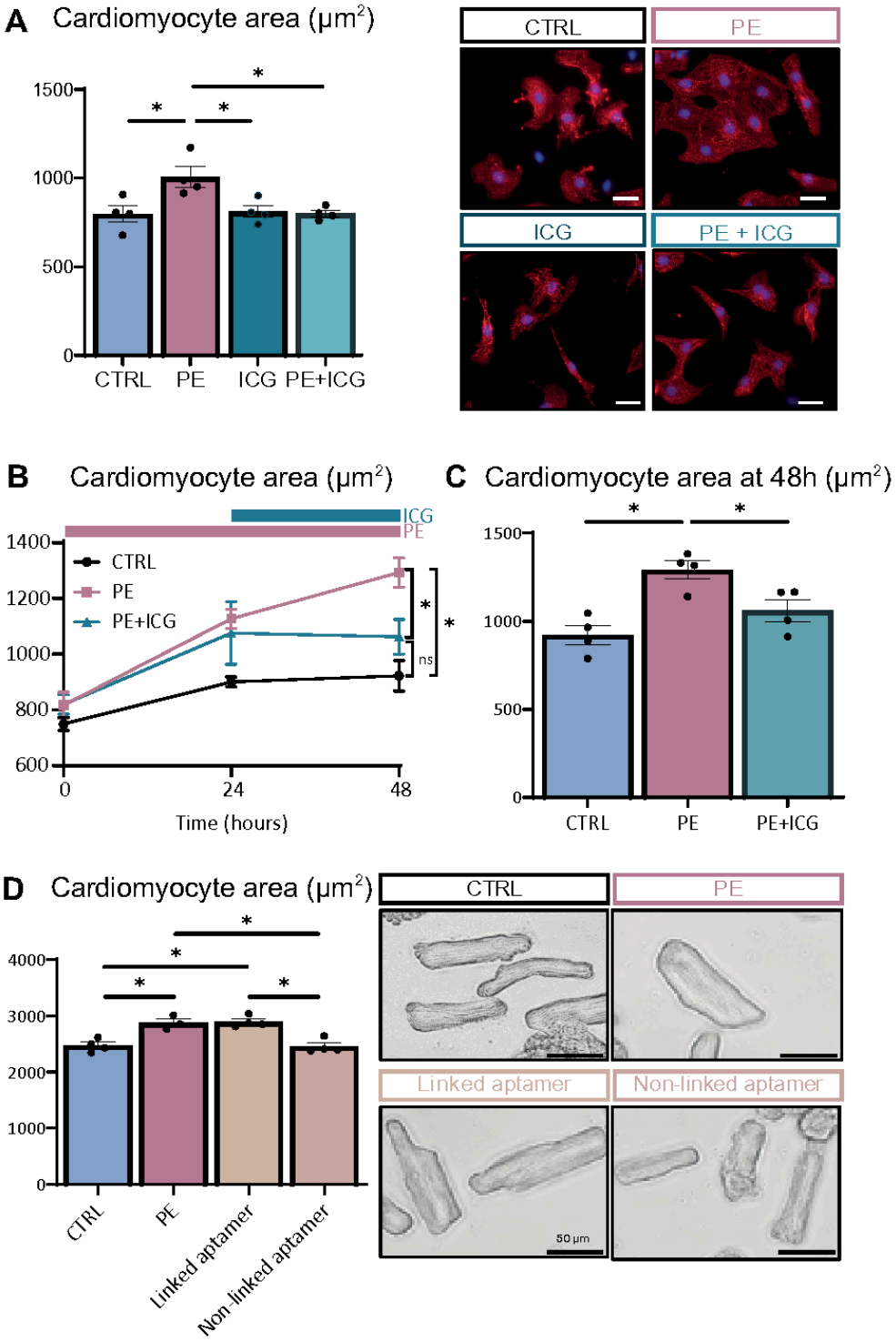


Figure 6

β-catenin activity controls cardiomyocytes hypertrophy. (**A**) Quantification of cell area in neonatal rat ventricular myocytes (NRVMs) treated or not with PE for 24 h, in the presence or absence of ICG-001

(n=4). Cell area was measured after α-actinin immunostaining. Scale bar, 40 μm. (**B,C**) NRVMs were first treated with PE for 24 h to induce hypertrophy, followed by ICG-001 treatment for an additional 24 h. Cell area was analyzed after α-actinin immunostaining. (**C**) Quantification of cell size 48 h after initial PE treatment, including 24 h of ICG-001 exposure. (**D**) Quantification of cell area in adult cardiomyocytes treated or not with PE for 48h. In parallel, cells were treated for 48h with either linked aptamer (promoting β-catenin O-GlcNAcylation) or the non-linked control aptamer. Cell area was measured after the treatments. Each point represents an independent biological replicate, with an average of 100–200 cells analyzed per condition for each replicate. Data are represented ± SEM. Statistical analyses are performed using one-way ANOVA followed Bonferroni post hoc test (**A,C,D**) or two-way ANOVA followed Bonferroni post hoc test (**B**). * Significant difference between groups.

Supplementary Files

This is a list of supplementary files associated with this preprint. Click to download.

- supplemental.pdf